^{99m}Tc-N-DBODC5, a New Myocardial Perfusion Imaging Agent with Rapid Liver Clearance: Comparison with ^{99m}Tc-Sestamibi and ^{99m}Tc-Tetrofosmin in Rats

Kengo Hatada, MD[1]; Laurent M. Riou, PhD[1]; Mirta Ruiz, MD[1]; Yoshihiro Yamamichi[2]; Adriano Duatti, PhD[3]; Ronaldo L. Lima, MD[1]; Allen R. Goode, MS[1]; Denny D. Watson, PhD[1]; George A. Beller, MD[1]; and David K. Glover, PhD[1]

[1]Experimental Cardiology Laboratory, Cardiovascular Division, Department of Internal Medicine, University of Virginia Health System, Charlottesville, Virginia; [2]Research and Development Division, Nihon Medi-Physics Co., Ltd., Sodegaura, Chiba, Japan; and [3]Laboratory of Nuclear Medicine, Department of Radiological Sciences, University of Ferrara, Ferrara, Italy

^{99m}Tc-[bis (dimethoxypropylphosphinoethyl)-ethoxyethylamine (PNP5)]-[bis (*N*-ethoxyethyl)-dithiocarbamato (DBODC)] nitride (N-PNP5-DBODC or N-DBODC5) is a new monocationic myocardial perfusion tracer. We sought to compare the myocardial uptake and clearance kinetics and organ biodistribution of ^{99m}Tc-N-DBODC5 with ^{99m}Tc-sestamibi and ^{99m}Tc-tetrofosmin. **Methods:** Seventy-five anesthetized Sprague–Dawley rats were injected intravenously with 22.2–29.6 MBq ^{99m}Tc-N-DBODC5 ($n = 25$), ^{99m}Tc-sestamibi ($n = 25$), or ^{99m}Tc-tetrofosmin ($n = 25$). Rats were euthanized at either 2, 10, 20, 30, or 60 min after injection and γ-well counting was performed on excised organ (heart, lung, and liver) and blood samples. In 3 additional rats, serial in vivo whole-body γ-camera imaging with each tracer was performed. **Results:** ^{99m}Tc-N-DBODC5 cleared rapidly from the blood pool. At 2 min after injection, ^{99m}Tc-N-DBODC5 blood activity was significantly lower than either ^{99m}Tc-sestamibi or ^{99m}Tc-tetrofosmin ($P < 0.01$) and remained lower over 60 min. Myocardial ^{99m}Tc-N-DBODC5 uptake was rapid (2.9% ± 0.1% injected dose/g at 2 min), and there was no significant clearance over 60 min, similar to ^{99m}Tc-sestamibi and ^{99m}Tc-tetrofosmin. All 3 tracers exhibited rapid lung clearance. Importantly, ^{99m}Tc-N-DBODC5 cleared more rapidly from the liver than either ^{99m}Tc-sestamibi or ^{99m}Tc-tetrofosmin. As early as 30 min after injection, ^{99m}Tc-N-DBODC5 heart-to-liver ratio was 5.7 ± 1.0 versus 1.6 ± 0.1 and 2.9 ± 0.3 for ^{99m}Tc-sestamibi and ^{99m}Tc-tetrofosmin ($P < 0.05$). By 60 min, ^{99m}Tc-N-DBODC5 heart-to-liver ratio further increased to 18.4 ± 2.0 compared with 2.6 ± 0.2 and 5.8 ± 0.7 for ^{99m}Tc-sestamibi and ^{99m}Tc-tetrofosmin ($P < 0.001$). The rapid blood pool, lung, and liver clearance of ^{99m}Tc-N-DBODC5 resulted in excellent-quality myocardial images within 30 min after injection. **Conclusion:** ^{99m}Tc-N-DBODC5 is a promising new myocardial perfusion tracer with superior biodistribution properties. The rapid ^{99m}Tc-N-DBODC5 liver clearance may shorten the duration of imaging protocols by allowing earlier image acquisition and may markedly reduce the problem of photon scatter from the liver into the inferoapical wall on myocardial images.

Key Words: ^{99m}Tc-N-DBODC5; myocardial perfusion imaging; organ biodistribution; liver clearance

J Nucl Med 2004; 45:2095–2101

Single-photon myocardial perfusion imaging agents labeled with ^{99m}Tc have been developed with properties better suited for γ-camera imaging than ^{201}Tl because of the higher photopeak and shorter half-life of ^{99m}Tc. Cationic ^{99m}Tc complexes, ^{99m}Tc-sestamibi (*1*) and ^{99m}Tc-tetrofosmin (*2,3*), are routinely used for clinical imaging with their favorable myocardial uptake and retention properties (*4*). Neutrally charged ^{99m}Tc complexes, ^{99m}Tc-teboroxime (*1,5*) and ^{99m}Tc-N-NOET (*6,7*), exhibit better flow-extraction properties at high flows compared with these cationic agents and have complete redistribution similar to ^{201}Tl (*8*). ^{99m}Tc-teboroxime is not routinely used because of its very rapid myocardial clearance kinetics (*9,10*), whereas ^{99m}Tc-N-NOET, the first reported compound characterized by the presence of a terminal technetium–nitrogen multiple bond (*6*), has not yet been approved for clinical imaging.

Although the physical properties of ^{99m}Tc are better suited than ^{201}Tl for γ-camera imaging, the organ biodistribution properties of these ^{99m}Tc-labeled tracers remain suboptimal for myocardial perfusion imaging. Interfering abdominal activity resulting from intense liver or gastrointestinal uptake is often observed for prolonged periods with these ^{99m}Tc-labeled agents because of their prominent hepatobiliary excretion (*11,12*). In particular, because of its close proximity to the heart, prolonged high liver uptake can

Received Aug. 6, 2004; revision accepted Aug. 11, 2004.

For correspondence or reprints contact: David K. Glover, PhD, Cardiovascular Division, Department of Internal Medicine, University of Virginia Health System, P.O. Box 800500, Charlottesville, VA 22908-0500.

E-mail: dglover@virginia.edu

make it difficult to accurately assess myocardial perfusion, particularly in the inferior or inferoapical left ventricular wall (*13–18*). Therefore, it is important to develop new tracers with improved organ biodistribution properties, with less liver uptake.

^{99m}Tc-[bis (dimethoxypropylphosphinoethyl)-ethoxyethylamine (PNP5)]-[bis (*N*-ethoxyethyl)-dithiocarbamato (DBODC)] nitride (N-PNP5-DBODC or N-DBODC5) is a new class nitrido ^{99m}Tc agent that is currently under investigation (*19,20*). The core of this molecule consists of ^{99m}Tc triple bonded to nitrogen, and it is highly lipophilic, similar to ^{99m}Tc-N-NOET (*19*). However, unlike ^{99m}Tc-N NOET, which is a neutral molecule, ^{99m}Tc-N-DBODC5 is monocationic, like ^{99m}Tc-sestamibi and ^{99m}Tc-tetrofosmin. Accordingly, the goal of this experimental study was to determine the organ biodistribution kinetics of ^{99m}Tc-N-DBODC5 in comparison with the existing ^{99m}Tc-labeled cationic agents, ^{99m}Tc-sestamibi and ^{99m}Tc-tetrofosmin.

MATERIALS AND METHODS

All experiments were performed with the approval of the University of Virginia Animal Care and Use Committee in compliance with the position of the American Heart Association on the use of research animals.

Biodistribution Study of ^{99m}Tc-Labeled Agents in Rats

The protocol of the present study is shown in Figure 1. Seventy-five Sprague–Dawley rats (200–250 g) were anesthetized with an intraperitoneal injection of either sodium pentobarbital (30 mg/kg) or a mixture of ketamine (80 mg/kg) and xylazine (19 mg/kg). A saphenous vein was exposed and 22.2–29.6 MBq of either ^{99m}Tc-N-DBODC5 ($n = 25$), ^{99m}Tc-sestamibi ($n = 25$), or ^{99m}Tc-tetrofosmin ($n = 25$) were injected. For each of the 3 tracers, the 25 rats were subdivided into 5 groups according to timing of euthanasia after tracer injection. The subgrouped animals ($n = 5$ for each subgroup) were euthanized at either 2, 10, 20, 30, or 60 min after injection. Samples of blood and organs (excised heart, lung, and liver tissues) were collected in preweighed containers. Tracer activity in each sample was determined using a γ-well scintillation counter (MINAXI 5550; Packard Instruments) with standard window settings for ^{99m}Tc (120–160 keV). The tissue counts were corrected for background and decay, and the activity in each organ sample was calculated as a percentage of the total injected dose.

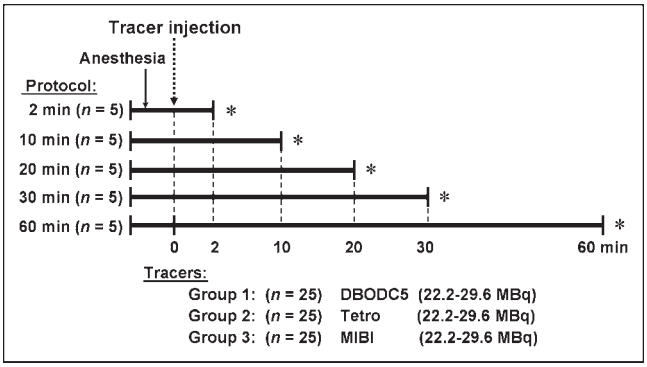

FIGURE 1. Experimental protocol ($n = 75$). DBODC5 = ^{99m}Tc-N-DBODC5; Tetro = ^{99m}Tc-tetrofosmin; MIBI = ^{99m}Tc-sestamibi. *Euthanasia; blood and tissue sampling.

In Vivo Whole-Body γ-Camera Imaging

To compare the tracer uptake and washout kinetics from the same animals and the same organs (heart, lung, liver) over time, serial in vivo γ-camera imaging was also performed in 9 additional anesthetized rats. Either 37.7–48.1 MBq of ^{99m}Tc-N-DBODC5 ($n = 3$), ^{99m}Tc-sestamibi ($n = 3$), or ^{99m}Tc-tetrofosmin ($n = 3$) was injected via a saphenous vein, after which the rats were placed supine directly on the surface of the low-energy, high-resolution collimator of a γ-camera (Digirad 20200tc Imager). In vivo whole-body images were acquired at 2, 30, and 60 min after injection using a 15% window centered on the 140-keV ^{99m}Tc photopeak. Image acquisition time was 5 min at each time point, resulting in approximately 0.4×10^6 counts in each image. The images were then quantified by regions of interest drawn on the heart, lung, and liver regions on each image.

Preparation of ^{99m}Tc-N-DBODC5

A dose of ^{99m}Tc-N-DBODC5 was synthesized with a lyophilized kit formulation as previously described by Boschi et al. (*20*). An aliquot of 1.0 mL of Na-^{99m}Tc-O_4 (50.0 MBq to 4.5 GBq) was added to a vial containing 5.0 mg of succinate dehydrogenase, 5.0 mg of ethylenediaminetetraacetic acid , 0.1 mg of $SnCl_2 \cdot 2H_2O$, and 1.0 mL of phosphate buffer (0.1 mol/dm^3) in a freeze-dried form. The resulting solution was kept at room temperature for 30 min. The contents of a second lyophilized vial consisting of 3.5 mg of PNP5, 3.5 mg of DBODC, and 3.5 mg of γ-cyclodextrin were reconstituted with 1.75 mL of saline. Then, 1.0 mL of the resulting solution was withdrawn from the second vial and added to the first vial, which was heated at 100°C for 15 min. The ^{99m}Tc-sestamibi and ^{99m}Tc-tetrofosmin doses were obtained from a local commercial radiopharmacy.

Purification and Quality Control of ^{99m}Tc-N-DBODC5

A cation exchange C-18 Sep-Pak cartridge (Waters) was activated with 5 mL of ethanol followed by 5 mL of deionized water. Then, the reaction solution containing the final ^{99m}Tc complex, ^{99m}Tc-N-DBODC5, was diluted with 8.0 mL of deionized water and passed through the activated cartridge. Approximately 60% of the initial activity was retained on the cartridge. After washing the cartridge with 20 mL of deionized water and 3 mL of an 80:20 mixture of ethanol (2.4 mL) and water (0.6 mL), the complex was recovered by passing 1.0 mL of a mixture of ethanol and an aqueous solution of NBu_4Br (0.1 mol/L) (90:10). Before injection, the radiochemical purity of all preparations was determined by thin-layer chromatography technique. The labeling efficiency of ^{99m}Tc-N-DBODC5 was greater than 96% in each experiment.

Data and Statistical Analysis

All statistical computations were made using SYSTAT software (SYSTAT Inc.). The results were expressed as the mean ± SEM. Differences between means within a group and difference between the 3 groups were assessed using a 1-way ANOVA (biodistribution data from γ-well counting) or a 2-way ANOVA (quantitative data from serial in vivo imaging), with P values < 0.05 considered significant. Nonlinear regression on liver washout kinetic data and

TABLE 1
^{99m}Tc-N-DBODC5 Biodistribution in Rats

Organ	%ID/g (mean ± SEM)				
	2 min	10 min	20 min	30 min	60 min
Blood	0.15 ± 0.01	0.02 ± 0.00*	0.02 ± 0.01*	0.01 ± 0.00*	0.01 ± 0.00*
Heart	2.98 ± 0.08	2.79 ± 0.09	3.04 ± 0.52	2.81 ± 0.13	2.95 ± 0.08
Lungs	1.18 ± 0.06	0.83 ± 0.04*	0.93 ± 0.07*	0.53 ± 0.02*	0.39 ± 0.02*
Liver	3.10 ± 0.17	1.78 ± 0.15	1.55 ± 0.19*	0.54 ± 0.08*	0.17 ± 0.02*
Heart/lung	2.56 ± 0.15	3.38 ± 0.19†	3.31 ± 0.61*	5.30 ± 0.26*	7.66 ± 0.35*
Heart/liver	0.97 ± 0.06	1.61 ± 0.15	2.13 ± 0.49*	5.68 ± 0.97	18.35 ± 2.03*

*$P < 0.01$ vs. 2-min time point.
†$P < 0.05$ vs. 2-min time point.
$n = 5$ for each time point; Heart/lung = heart-to-lung activity ratio; heart/liver = heart-to-liver activity ratio.

calculation of the $T_{1/2}$ parameter for all 3 tracers was performed using Prism software (Graphpad Software, Inc.).

RESULTS

Biodistribution in Rats

Organ biodistribution data for ^{99m}Tc-N-DBODC5 over time are presented in Table 1 and Figures 2–7. No statistically significant differences were observed in the injected doses among the 3 tracers. As shown in Figure 2, ^{99m}Tc-N-DBODC5 exhibited rapid clearance from the blood pool. As early as 2 min after injection, the blood activity for ^{99m}Tc-N-DBODC5 was less than the other 2 tracers and remained lower for 30 min. At 60 min, ^{99m}Tc-N-DBODC5 blood activity was still less than that of ^{99m}Tc-sestamibi. The bar graph in Figure 3 compares the amount of myocardial uptake of the 3 tracers at the various time points. As shown, myocardial ^{99m}Tc-N-DBODC5 uptake was rapid, and there was no significant clearance over 60 min, similar to ^{99m}Tc-tetrofosmin and ^{99m}Tc-sestamibi. Figure 4 compares heart-to-lung uptake ratios from γ-well counting. All 3 tracers exhibited rapid lung clearance. At 2 min, however, the mean heart-to-lung ratio for ^{99m}Tc-N-DBODC5 was higher than that of ^{99m}Tc-sestamibi, and the ratio increased from 2.6 to 7.7 over 60 min ($P < 0.001$ vs. 2 min). On in vivo images, lung clearance was rapid and comparable for all 3 tracers.

Importantly, ^{99m}Tc-N-DBODC5 exhibited more rapid liver clearance than either ^{99m}Tc-tetrofosmin or ^{99m}Tc-sestamibi. As shown in Figure 5A, as early as 30 min after injection, the mean heart-to-liver ratio for ^{99m}Tc-N-DBODC5 from γ-well counting (5.7 ± 1.0) was higher than for either ^{99m}Tc-tetrofosmin (2.9 ± 0.3) or ^{99m}Tc-sestamibi (1.6 ± 0.1) ($P < 0.05$ vs. ^{99m}Tc-tetrofosmin, and $P < 0.01$ vs. ^{99m}Tc-sestamibi). Furthermore, the mean heart-to-liver ratio for ^{99m}Tc-N-DBODC5 increased from 5.7 at 30 min to 18.4 by 60 min, further widening the difference between ^{99m}Tc-N-DBODC5 and the other 2 ^{99m}Tc-agents (5.8 ± 0.7 and 2.6 ± 0.2 for ^{99m}Tc-tetrofosmin and ^{99m}Tc-sestamibi;

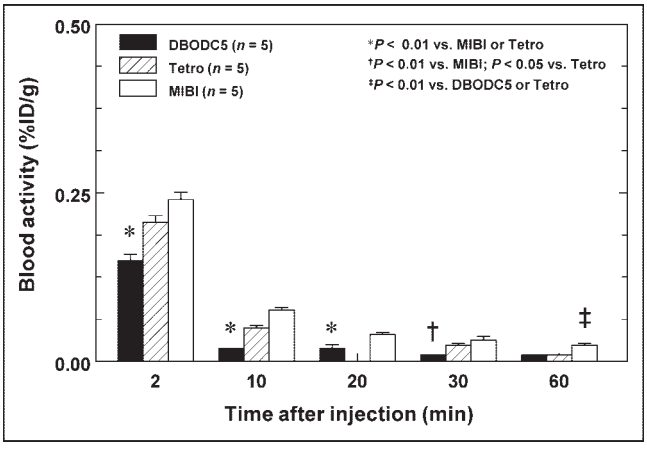

FIGURE 2. Comparison of blood activity over time. ^{99m}Tc-N-DBODC5 exhibited more rapid clearance from blood pool. DBODC5 = ^{99m}Tc-N-DBODC5; Tetro = ^{99m}Tc-tetrofosmin; MIBI = ^{99m}Tc-sestamibi.

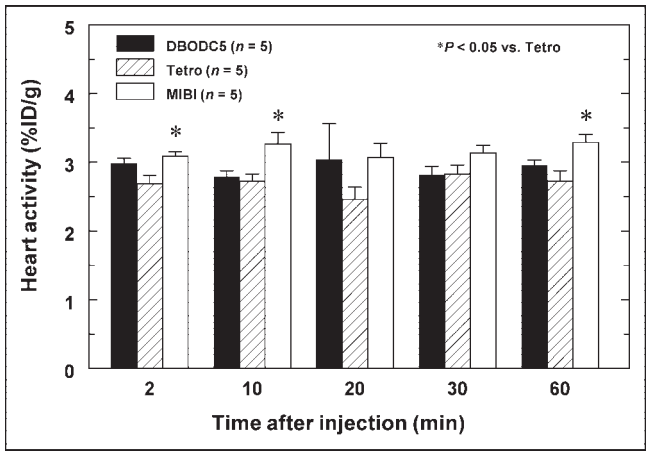

FIGURE 3. Comparison of heart activity over time from γ-well counting. There is no significant clearance of ^{99m}Tc-N-DBODC5 from heart over 60 min, similarly to the other cationic ^{99m}Tc-labeled tracers. DBODC5 = ^{99m}Tc-N-DBODC5; Tetro = ^{99m}Tc-tetrofosmin; MIBI = ^{99m}Tc-sestamibi.

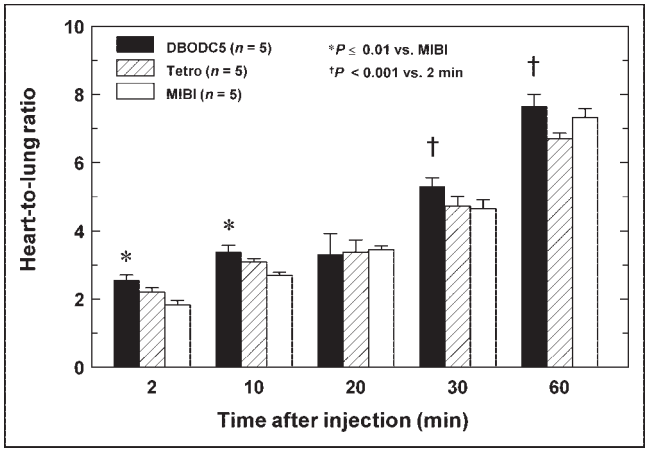

FIGURE 4. Comparison of heart-to-lung activity ratios over time from γ-well counting. All 3 tracers exhibited rapid lung clearance; however, at 2 min the mean heart-to-lung ratios for ^{99m}Tc-N-DBODC5 were higher than those for ^{99m}Tc-sestamibi and increased significantly over 60 min. DBODC5 = ^{99m}Tc-N-DBODC5; Tetro = ^{99m}Tc-tetrofosmin; MIBI = ^{99m}Tc-sestamibi.

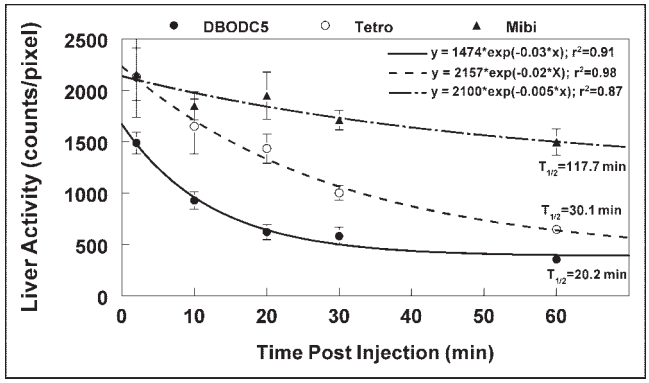

FIGURE 6. Liver clearance kinetics for the 3 ^{99m}Tc-labeled agents. Tracer activities were determined from a region of interest placed on liver on in vivo images. $T_{1/2}$ value calculated from monoexponential curve fitting for DBODC5 clearance was approximately 1.5 and 6 times faster than for Tetro and Mibi, respectively. DBODC5 = ^{99m}Tc-N-DBODC5; Tetro = ^{99m}Tc-tetrofosmin; MIBI = ^{99m}Tc-sestamibi.

$P < 0.001$, respectively). As shown in Figure 5B, the significantly faster liver clearance of ^{99m}Tc-N-DBODC5 was also observed by in vivo image quantification. Figure 6 compares the liver clearance kinetics among these 3 ^{99m}Tc-labeled tracers. Liver activity was determined from a region of interest placed over the liver on the in vivo images. Nonlinear regression analysis using a monoexponential curve fit revealed that ^{99m}Tc-N-DBODC5 cleared from the liver approximately 1.5 times faster than ^{99m}Tc-tetrofosmin and 6 times faster than ^{99m}Tc-sestamibi. Similar results were obtained from the analysis of the γ-well counting of liver samples from rats euthanized at different time points ($P <$ 0.01, respectively).

In Vivo γ-Camera Imaging

Figure 7 displays in vivo whole-body planar images acquired at different time points after tracer injection. On all initial images acquired at 2 min after injection, very high liver uptake can be seen adjacent to the heart. By 30 min after injection, ^{99m}Tc-N-DBODC5 liver uptake visibly decreased and nearly disappeared at 60 min after injection, whereas high liver uptake still can be seen on the ^{99m}Tc-sestamibi image at this time point. The ^{99m}Tc-tetrofosmin liver uptake was intermediate between that of ^{99m}Tc-N-DBODC5 and ^{99m}Tc-sestamibi at 60 min.

DISCUSSION

Accurate determination of myocardial perfusion status and cellular integrity has major clinical and prognostic

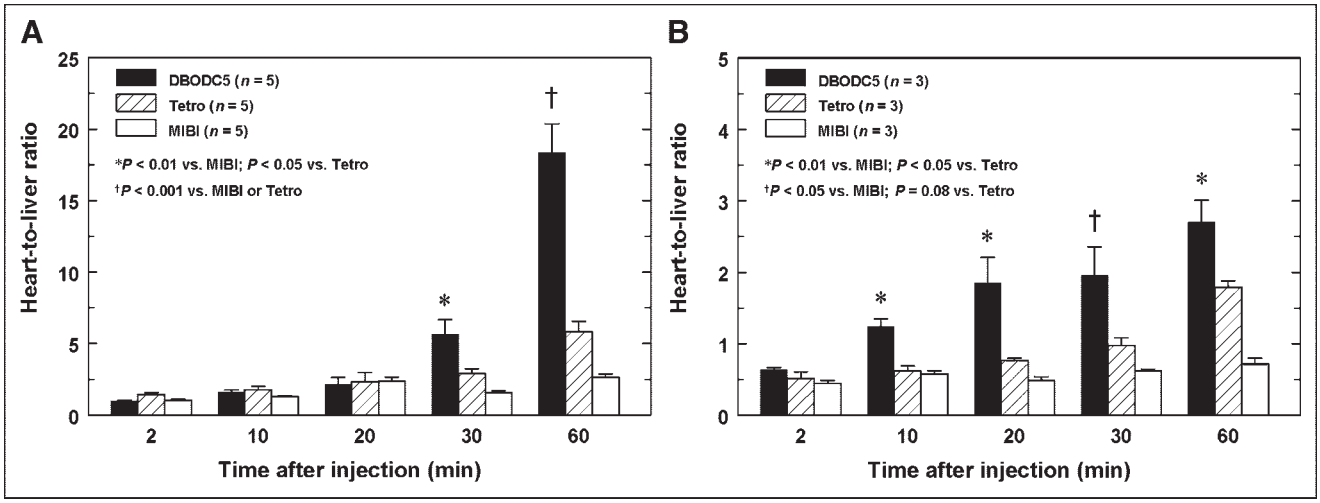

FIGURE 5. Comparison of heart-to-liver activity ratios over time from γ-well counting (A) and in vivo image quantification (B). Faster liver clearance of ^{99m}Tc-N-DBODC5, compared with the other ^{99m}Tc-labeled agents, was observed with both ex vivo γ-well counting and in vivo whole-body imaging. DBODC5 = ^{99m}Tc-N-DBODC5; Tetro = ^{99m}Tc-tetrofosmin; MIBI = ^{99m}Tc-sestamibi.

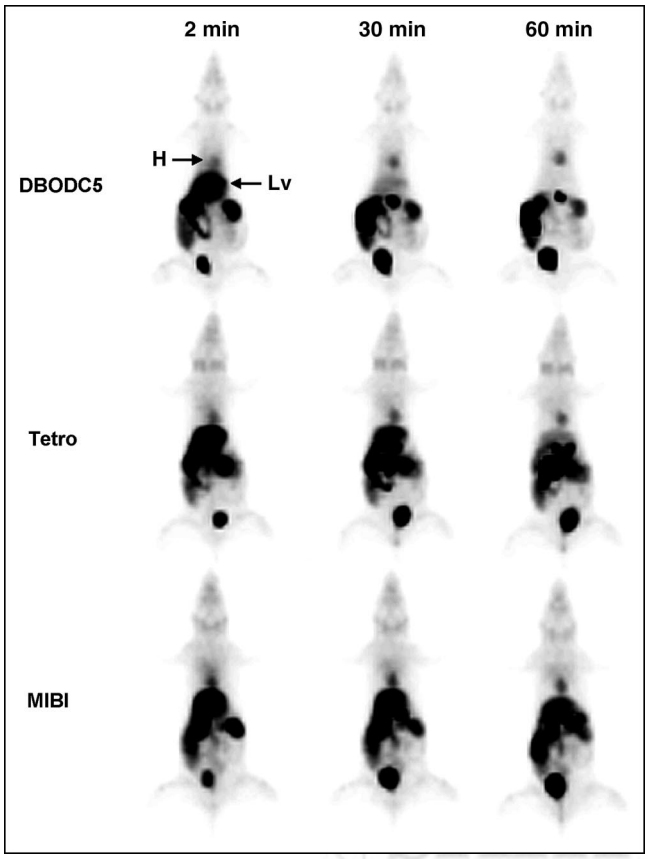

FIGURE 7. Serial in vivo whole-body images for ^{99m}Tc-N-DBODC5 (top), ^{99m}Tc-tetrofosmin (middle), and ^{99m}Tc-sestaibi (bottom). Persistent heart uptake can be seen with all of the tracers, whereas ^{99m}Tc-N-DBODC5 liver uptake cleared more rapidly than the other 2 tracers. DBODC5 = ^{99m}Tc-N-DBODC5; Tetro = ^{99m}Tc-tetrofosmin; MIBI = ^{99m}Tc-sestamibi; H = heart; Lv = liver.

importance and may affect critical therapeutic decision-making in patients with ischemic heart disease. Over the past 2 decades, there has been a great deal of effort to develop ^{99m}Tc-labeled myocardial perfusion tracers for clinical γ-camera imaging. However, despite the more favorable physical properties of ^{99m}Tc compared with ^{201}Tl, at present none of the ^{99m}Tc-labeled agents that have been approved for clinical use has ideal biodistribution properties.

In this experimental study, we found that a new nitrido class ^{99m}Tc agent, ^{99m}Tc-N-DBODC5, exhibits high heart uptake and novel biodistribution kinetics with its rapid liver clearance in anesthetized rat models. The quantitative biodistribution data for ^{99m}Tc-N-DBODC5 are consistent with the first published findings of favorable biodistribution kinetics of this new ^{99m}Tc-labeled agent (*19*). Consistent with the results of the quantitative organ biodistribution, the present study compares for the first time serial in vivo whole-body planar images of ^{99m}Tc-N-DBODC5 with the existing agents, ^{99m}Tc-sestamibi and ^{99m}Tc-tetrofosmin. The more rapid liver clearance as well as the relatively high heart uptake yielded high-quality in vivo ^{99m}Tc-N-DBODC5 images. These findings suggest that ^{99m}Tc-N-DBODC5 is a promising new agent and may allow for more accurate assessment of myocardial perfusion with less photon scatter from the liver. This may provide better accuracy for detection of coronary artery disease and for myocardial viability assessment.

With clinical γ-camera imaging using ^{99m}Tc-labeled myocardial perfusion tracers, interfering abdominal activity due to intense liver or gastrointestinal uptake may make it difficult to interpret the heart activity, particularly in the inferior or inferoapical left ventricular wall (*13–18*). High liver uptake is frequently observed with rest or pharmacologic stress studies (*14*) and results from the prominent hepatobiliary excretion of the lipophilic ^{99m}Tc-labeled tracers (*11,12*). Prolonged intense abdominal activity adjacent to the heart can lead to a paradoxical decrease of counts in the inferior wall in the absence of perfusion abnormalities (*13*). Test specificity in detection of coronary artery disease could be affected by a false-positive inferior wall defect on stress and rest images (*14*). This intense liver activity has been reported for both ^{99m}Tc-sestamibi (*21*) and ^{99m}Tc-tetrofosmin (*3*).

To overcome this problem, several technical attempts have been undertaken in clinical imaging. Early image acquisition after tracer injection has been advised to prevent intestinal artifacts (*22*), while late image acquisition is recommended to avoid liver artifacts (*17,23*). These suggestions are based on the fact that, with hepatobiliary clearance, the activity of the excreted tracer moves from the liver and gallbladder to the gastrointestinal area over time (*24*). Although gastrointestinal activity can be reduced and distanced from the heart by filling the stomach before image acquisition (*24–26*), it is more important to reduce the liver uptake or to stimulate the liver clearance to achieve high-quality myocardial perfusion image acquisition. Although giving high-lipid foods to stimulate the gallbladder and reduce liver activity has been attempted, Hurwitz et al. demonstrated using milkshake ingestion that this measure was insufficient to reduce intense liver activity (*25*). The measure was effective only in reduction of interfering intestinal activity on the heart image by increasing the volume of the stomach with fluid (*25*).

Other means of reducing artifacts caused by high liver uptake have involved modifications to image reconstruction algorithms. Image reconstruction via filtered backprojection is the current standard in clinical myocardial perfusion imaging (*27*). This process is well known to cause artifactual decreased myocardial wall uptake if the liver activity is greater than the heart with ^{99m}Tc myocardial imaging (*28*). With phantom measurements, Germano et al. suggested higher frequency cutoffs in prereconstruction filters, if count statistics are good and liver uptake is high (*15*). Nuyts et al. emphasized the importance of accurate attenuation

correction in the left ventricular wall counting rate (*16*). The authors also demonstrated that 360° reconstruction, in comparison with 180° reconstruction, reduces the differences in attenuation between the different projections, therefore reducing the reconstruction artifacts (*16*). However, despite these efforts in both basic and clinical studies, photon scatter from extremely high liver activity on attenuation-corrected images is still an unresolved problem (*29*). To date, no technique is commonly available to completely overcome abdominal image artifacts. Thus, developing new ^{99m}Tc-labeled myocardial agents that exhibit more favorable organ biodistribution properties, with less liver uptake without reducing myocardial uptake would be a great advance.

Biochemical mechanisms for the markedly rapid liver clearance of ^{99m}Tc-N-DBODC5 remain unknown. However, one potential explanation is the lipophilic character and the electronic charge of the tracer. The lower the lipophilicity of a compound the lower the initial uptake in the liver (*30,31*). Boschi et al. demonstrated that substitution of ^{99m}Tc-N-DBODC5 with a similar monocationic nitride ^{99m}Tc complex, which has higher lipophilic profile, caused an increased liver accumulation of the tracer (*20*).

In contrast to the marked difference in liver clearance kinetics, the heart uptake of this new tracer was comparable to that seen with the other cationic ^{99m}Tc-labeled tracers, ^{99m}Tc-sestamibi and ^{99m}Tc-tetrofosmin. The myocardial uptake of ^{99m}Tc-sestamibi and ^{99m}Tc-tetrofosmin have been reported to be driven by electropotential gradient according to the Nernst equation, and these tracers exhibit prolonged accumulation in mitochondria (*32–34*). Because ^{99m}Tc-N-DBODC5 is also highly lipophilic and monocationic, it is possible that the mechanism for myocardial uptake and washout of this tracer is similar to ^{99m}Tc-sestamibi and ^{99m}Tc-tetrofosmin. Further studies are necessary to determine the exact mechanism for myocardial uptake of this novel tracer.

The main findings of this rat biodistribution study were, first, high myocardial uptake of ^{99m}Tc-N-DBODC5 with slow clearance similar to that of ^{99m}Tc-sestamibi and ^{99m}Tc-tetrofosmin and, second, rapid blood, lung, and especially liver clearance of ^{99m}Tc-N-DBODC5 allowing for excellent-quality in vivo heart images as early as 30 min after injection.

One clinical implication of the present study is that the fast ^{99m}Tc-N-DBODC5 liver clearance kinetics may significantly reduce photon scatter from the liver into the inferior and inferoapical walls on myocardial perfusion images, thereby reducing artifacts and potentially improving the diagnostic accuracy for the detection of coronary artery disease compared with the other ^{99m}Tc-labeled perfusion agents. Moreover, these novel biodistribution properties might shorten the duration of imaging protocols, allowing for earlier image acquisition.

CONCLUSION

^{99m}Tc-N-DBODC5 is a promising new myocardial perfusion imaging agent with superior biodistribution properties. For clinical imaging, the more rapid liver clearance could give the new tracer an advantage over the other ^{99m}Tc-labeled tracers.

ACKNOWLEDGMENT

This experimental study was funded by a research grant from Nihon Medi-Physics Co., Ltd. YoshihiroYamamichi is employed by NMP. Dr. Adriano Duatti has a financial interest in ^{99m}Tc-N-DBODC5.

REFERENCES

1. Beller GA, Watson DD. Physiological basis of myocardial perfusion imaging with the technetium 99m agents. *Semin Nucl Med.* 1991;21:173–181.
2. Kelly JD, Forster AM, Higley B, et al. Technetium-99m-tetrofosmin as a new radiopharmaceutical for myocardial perfusion imaging. *J Nucl Med.* 1993;34: 222–227.
3. Nakajima K, Taki J, Shuke N, Bunko H, Takata S, Hisada K. Myocardial perfusion imaging and dynamic analysis with technetium-99m tetrofosmin. *J Nucl Med.* 1993;34:1478–1484.
4. Schwaiger M, Melin J. Cardiological applications of nuclear medicine. *Lancet.* 1999;354:661–666.
5. Leppo JA, DePuey EG, Johnson LL. A review of cardiac imaging with sestamibi and teboroxime. *J Nucl Med.* 1991;32:2012–2022.
6. Pasqualini R, Duatti A, Bellande E, et al. Bis (dithiocarbamato) nitrido technetium-99m radiopharmaceuticals: a class of neutral myocardial imaging agents. *J Nucl Med.* 1994;35:334–341.
7. Fagret D, Ghezzi C, Vanzetto G. ^{99m}Tc-N-NOET imaging for myocardial perfusion: can it offer more than we already have? *J Nucl Med.* 2001;42:1395–1396.
8. Vanzetto G, Calnon DA, Ruiz M, et al. Myocardial uptake and redistribution of ^{99m}Tc-N-NOET in dogs with either sustained coronary low flow or transient coronary occlusion: comparison with ^{201}Tl and myocardial blood flow. *Circulation.* 1997;96:2325–2331.
9. Narra RK, Nunn AD, Kuczynski BL, Feld T, Wedeking P, Eckelman WC. A neutral technetium-99m complex for myocardial imaging. *J Nucl Med.* 1989;30: 1830–1837.
10. Seldin DW, Johnson LL, Blood DK, et al. Myocardial perfusion imaging with technetium-99m SQ30217: comparison with thallium-201 and coronary anatomy. *J Nucl Med.* 1989;30:312–319.
11. O'Connor MK, Kelly BJ. Evaluation of techniques for the elimination of "hot" bladder artifacts in SPECT of the pelvis. *J Nucl Med.* 1990;31:1872–1875.
12. Wackers FJ, Berman DS, Maddahi J, et al. Technetium-99m hexakis 2-methoxyisobutyl isonitrile: human biodistribution, dosimetry, safety, and preliminary comparison to thallium-201 for myocardial perfusion imaging. *J Nucl Med.* 1989;30:301–311.
13. Higley B, Smith FW, Smith T, et al. Technetium-99m-1,2-bis [bis(2-ethoxyethyl) phosphino] ethan: biodistribution, dosimetry and safety of a new myocardial perfusion imaging agent. *J Nucl Med.* 1993;34:30–38.
14. Chua T, Kiat H, Germano G, et al. Rapid back to back adenosine stress/rest technetium-99m teboroxime myocardial perfusion SPECT using a triple-detector camera. *J Nucl Med.* 1993;34:1485–1493.
15. Germano G, Chua T, Kiat H, Areeda JS, Berman DS. A quantitative phantom analysis of artifacts due to hepatic activity in technetium-99m myocardial perfusion SPECT studies. *J Nucl Med.* 1994;35:356–359.
16. Nuyts J, Dupont P, Van den Maegdenbergh V, Vleugels S, Suetens P, Mortelmans L. A study of the liver-heart artifact in emission tomography. *J Nucl Med.* 1995;36:133–139.
17. Matsunari I, Tanishima Y, Taki J, et al. Early and delayed technetium-99m-tetrofosmin myocardial SPECT compared in normal volunteers. *J Nucl Med.* 1996;37:1622–1626.
18. Kailasnath P, Sinusas AJ. Comparison of Tl-201 with Tc-99m-labeled myocardial perfusion agents: technical, physiologic, and clinical issues. *J Nucl Cardiol.* 2001;8:482–498.
19. Boschi A, Bolzati C, Uccelli L, et al. A class of asymmetrical nitrido ^{99m}Tc

heterocomplexes as heart imaging agents with improved biological properties. *Nucl Med Commun.* 2002;23:689–693.
20. Boschi A, Uccelli L, Bolzati C, et al. Synthesis and biologic evaluation of monocationic asymmetric ^{99m}Tc-nitride heterocomplexes showing high heart uptake and improved imaging properties. *J Nucl Med.* 2003;44:806–814.
21. Okada RD, Glover D, Gaffney T, Williams S. Myocardial kinetics of technetium-99m-hexakis-2-methoxy-2-methylpropyl-isonitrile. *Circulation.* 1988;77:491–498.
22. Wackers FJT. Myocardial perfusion imaging. In: Sandler MP, Coleman RE, Wackers FJT, et al., eds. *Diagnostic Nuclear Medicine.* Philadelphia, PA: Williams and Wilkins; 1996:443–516.
23. Boz A, Gungor F, Karayalcin B, Yildiz A. The effects of solid food in prevention of intestinal activity in Tc-99m tetrofosmin myocardial perfusion scintigraphy. *J Nucl Cardiol.* 2003;10:161–167.
24. van Dongen AJ, van Rijk PP. Minimizing liver, bowel, and gastric activity in myocardial perfusion SPECT. *J Nucl Med.* 2000;41:1315–1317.
25. Hurwitz GA, Clark EM, Slomka PJ, Siddiq SK. Investigation of measures to reduce interfering abdominal activity on rest myocardial images with Tc-99m sestamibi. *Clin Nucl Med.* 1993;18:735–741.
26. Boz A, Karayalcin B. Which is better for inferior wall evaluation: a full or empty stomach? *J Nucl Med.* 1996;37:1916–1917.
27. Shepp L, Logan B. The fourier reconstruction of a head section. *IEEE Trans Nucl Sci.* 1974;21:21–43.
28. Germano G, Chua T, Areeda J, Kiat H, Berman D. Hepatic uptake creates artifactual defects in Tc-99m myocardial SPECT images: a quantitative phantom analysis [abstract]. *J Nucl Med.* 1993;34(suppl):189P.
29. Ficaro EP, Fessler JA, Shreve PD, Kritzman JN, Rose PA, Corbett JR. Simultaneous transmission/emission myocardial perfusion tomography: diagnostic accuracy of attenuation-corrected ^{99m}Tc-sestamibi single-photon emission computed tomography. *Circulation.* 1996;93:463–473.
30. Marmion ME, Woulfe SR, Neumann WL, Nosco DL, Deutsch E. Preparation and characterization of technetium complexes with schiff base and phosphine coordination. 1. Complexes of technetium-99g and -99m with substituted acac2en and trialkyl phosphines (where acac2en = N,N′-ethylenebis[acetylacetone iminato]). *Nucl Med Biol.* 1999;26:755–770.
31. Bolzati C, Uccelli L, Boschi A, et al. Synthesis of a novel class of nitrido Tc-99m radiopharmaceuticals with phosphino-thiol ligands showing transient heart uptake. *Nucl Med Biol.* 2000;27:369–374.
32. Piwnica-Worms D, Kronauge JF, Chiu ML. Uptake and retention of hexakis (2-methoxyisobutyl isonitrile) technetium(I) in cultured chick myocardial cells: mitochondrial and plasma membrane potential dependence. *Circulation.* 1990; 82:1826–1838.
33. Platts EA, North TL, Pickett RD, Kelly JD. Mechanism of uptake of technetium-tetrofosmin. I: uptake into isolated adult rat ventricular myocytes and subcellular localization. *J Nucl Cardiol.* 1995;2:317–326.
34. Younes A, Songadele JA, Maublant J, Platts E, Pickett R, Veyre A. Mechanism of uptake of technetium-tetrofosmin. II: uptake into isolated adult rat heart mitochondria. *J Nucl Cardiol.* 1995;2:327–333.